

PFC/JA-84-24

**Frequency Pulling and Bandwidth Measurements
of a 140 GHz Pulsed Gyrotron**

K.E. Kreischer, B.G. Danly, P. Woskoboinikow

W.J. Mulligan, and R.J. Temkin

Plasma Fusion Center
Massachusetts Institute of Technology
Cambridge, MA 02139

June 1984

This work was supported by the U.S. Department of Energy Contract No. DE-AC02-78ET51013.

By acceptance of this article, the publisher and/or recipient acknowledges the U.S. Government's right to retain a nonexclusive royalty-free licence in and to any copyright covering this paper.

**Frequency Pulling and Bandwidth Measurements
of a 140 GHz Pulsed Gyrotron**

**K.E. Kreischer, B.G. Danly, P. Woskoboinkow
W.J. Mulligan, and R.J. Temkin**

**Plasma Fusion Center
Massachusetts Institute of Technology
Cambridge, MA 02139**

June 1984

ABSTRACT

Accurate measurements of the emission frequency and bandwidth of a pulsed 140 GHz gyrotron have been made using a harmonic mixer system. This system has been used to measure the bandwidth of individual, 1 μ sec pulses of the gyrotron, to determine the dependence of the operating frequency on the cathode voltage and resonator magnetic field, to detect and identify second harmonic radiation, and to study multimode operation. Bandwidths as low as 3 MHz, which is the instrumental limit, have been observed. In addition, frequency pulling has been measured and compared with predictions based on linear and self-consistent nonlinear theory. It was found that linear theory is inadequate for describing the frequency characteristics of a gyrotron operating well above the starting current, while self-consistent nonlinear theory was in reasonable agreement with the experimental results. The small bandwidths and stable operating frequencies that were measured confirm the viability of the gyrotron as a millimeter and submillimeter source for plasma diagnostics.

I. INTRODUCTION

The gyrotron has proven to be a powerful source of millimeter and submillimeter radiation (Gaponov *et al.* 1981), and has been used extensively for electron cyclotron resonance heating of fusion plasmas. A variety of recent experiments, including research on T-10 (Alikaev *et al.* 1983) and PDX (Hsuan *et al.* 1984) have demonstrated effective coupling of the radiation to the plasma. In addition to bulk heating, gyrotrons are also being considered for initiation of the plasma as well as plasma stability. Recently, interest has developed in the potential of the gyrotron as an rf source for plasma diagnostics (Temkin *et al.* 1982b, Woskoboinikow *et al.* 1983, Fiks *et al.* 1984). Moderate to high powers (100 W to 100 kW) would be necessary for Thomson scattering from thermal or low level nonthermal plasma fluctuations, while modest powers (1 W to 100 W) would be sufficient for scattering from strong nonthermal fluctuations. Gyrotrons are capable of delivering both the high power and energy needed to obtain good signal to noise ratios. One such diagnostic system is presently being constructed for the TARA tandem mirror experiment (Cohn *et al.* 1983). Using a 1-10 kW, 140 GHz long pulse gyrotron, this experiment will measure scattering in the plugs from both ion cyclotron and ion acoustic waves.

In order to evaluate the potential of the gyrotron as a diagnostic source, a clear understanding of the emission characteristics of the device is required. Such investigations of the emission frequency have recently been conducted, including frequency detuning measurements in a low power gyrotron (Brand *et al.* 1983) and a comparison between self-consistent nonlinear theory and experimental results for a low Q, 35 GHz gyrotron operating in the $TE_{0,1,1}$ mode (Fliflet *et al.* 1982). The present study differs from previous work in that good agreement has been achieved between the theoretical and experimental efficiency in our device (Kreischer *et al.* 1984b). Under these conditions, the degree of

agreement between theory and experiment for frequency tuning provides an important additional test of the theoretical formalism.

In this paper, a detailed study of the emission frequency of a 140 GHz, pulsed gyrotron using a harmonic mixer system will be described. The mixer system, which is capable of measuring the frequency to within a few MHz, has allowed us to determine the bandwidth of the device and the dependence of the emission frequency on operating parameters such as cathode voltage and resonator magnetic field. In addition to confirming the viability of the high frequency gyrotron as a plasma diagnostic tool, these measurements have also provided a valuable insight into the operating characteristics of the device. By combining this data with measurements of the output power, total efficiency, and mode content, it has been possible to make direct comparisons between theory and experiment. In particular, frequency pulling resulting from variation of the magnetic field and beam current has been measured and compared with predictions based on both linear theory and self-consistent nonlinear theory. Such comparisons have been used to indirectly determine device parameters such as the total cavity Q .

Accurate measurement of the operating frequency can also be used to provide a better match of the rf window and transmission system to the output radiation. It has been found that component mismatches can result in distortions of the frequency pulling characteristics. They can therefore be identified and remedied. Such mismatches could be problematic in long pulse and cw devices because they could result in excessive localized heating due to trapped modes in the gyrotron and the output waveguide.

This paper will be organized in the following manner. In Section 2, a description of the 140 GHz gyrotron and the harmonic mixer system will be given. The experimental results will be presented in Section 3, including frequency pulling data for the $TE_{4,2,1}(127.3$

GHz), $TE_{2,3,1}$ (136.7 GHz), and $TE_{0,3,1}$ (139.5 GHz) modes. Calculation of the emission frequency based on both linear theory and self-consistent nonlinear theory will be outlined in Section 4 and compared with the experimental results. This comparison will show that linear theory is inadequate for describing the emission frequency when operating well above the starting current. Conclusions will be given in Section 5.

2. DESCRIPTION OF EXPERIMENT

The MIT 140 GHz gyrotron has been operational since early 1982 and has been tested over a wide range of parameters. The magnetic field has been varied from 4 to 7 T, and as a result of the dense spectrum of the relatively oversized cavity, a variety of fundamental modes have been excited from 120 to 200 GHz. In addition, second harmonic emission has been observed between 200 and 300 GHz, including the generation of 25 kW of output power at 241 GHz (Byerly *et al* 1984). A detailed description of the design and initial operation of the experiment can be found in an earlier paper (Temkin *et al.* 1982a). An extensive effort was subsequently made (Kreischer *et al.* 1984b) to understand and improve the operating characteristics of the device. This eventually led to total efficiencies as high as 36% and peak output powers of 175 kW in single mode operation. The best results have been achieved with isolated, asymmetric modes that are not hampered by mode competition, such as the $TE_{4,2,1}$ (127.3 GHz), $TE_{2,3,1}$ (136.7 GHz), and the $TE_{3,3,1}$ (155.6 GHz) modes.

A harmonic mixer system has been used to measure the operating frequency of the gyrotron to within a few MHz. This highly accurate and sensitive diagnostic has been able to detect both fundamental and second harmonic radiation over the full 100 to 300 GHz region in which emission has been observed. In addition, this system has the capability of responding to both weakly and strongly excited modes. The resolution of the mixer system greatly exceeds that available from millimeter wavemeters, which typically can measure frequencies to within ± 100 MHz. The mixer system also is capable of detecting weak parasitic modes excited simultaneously with a strong mode, modes that would probably be missed with a wavemeter. In contrast to Fabry-Perot interferometer scans, which require averaging over many pulses, the frequency measurements made with the mixer are on a

single shot, real time basis, and bandwidth measurements are unaffected by shot to shot variations of the gyrotron emission.

Figure 1 shows a simplified block diagram of the harmonic mixer system. The radiation which is generated in the gyrotron cavity is transmitted by an oversized circular waveguide to a Corning 7940 fused quartz window 0.554 cm thick. The radiation is then broadcast into free space. The receiving horn of the mixer system was situated in the far field of the radiation about 40 cm from the output waveguide. This minimizes possible feedback into the gyrotron. To ensure that the mixer is receiving the strongest possible rf signal, the horn was placed at an angle with respect to the waveguide axis corresponding to the main rf lobe, which in our experiment occurs at about 18°.

The incoming signal was analyzed by heterodyning it with the harmonic of a lower frequency local oscillator (LO) and then processing the resulting intermediate frequency (IF) in a surface acoustic wave (SAW) dispersive delay line. This same technique was previously used to perform real-time spectral analysis of far infrared lasers (Fetterman *et al.* 1979). In our experiment, either a Wavetek model 907A signal generator, which produces an rf signal between 7.0 and 12.4 GHz, or an Omniyig YIG tuned Gunn oscillator capable of generating 20-30 mW of power between 12 and 16 GHz, served as the LO source. The gyrotron signal was mixed in a broadband Hughes harmonic mixer, model 47448H, with the 10th to 14th harmonic of the LO in the case of fundamental radiation, while the 18th to 22nd harmonic was typically used for second harmonic emission. The LO frequency was monitored with an EIP frequency counter, model 548. After the IF signals generated in the mixer were amplified, the SAW filter was used to display those signals between 370 and 470 MHz on an oscilloscope. An rf switch in the IF circuit was used to gate a 250-300 ns portion of the 1-2 μ sec long gyrotron pulse. By varying the delay of this gate relative to

the gyrotron pulse, the gyrotron bandwidth and frequency could be analyzed at different times in the pulse.

The essential element of the mixer system is the SAW device, which is a LiNbO_3 dispersive delay line originally developed for use as a radar pulse expander and compressor. The input IF signal, which must be between 370 and 470 MHz, is delayed between 4 and 20.3 μsec . the amount of delay being a linear function of the IF frequency. Since higher IF signals lead to shorter delays in our SAW filter, it is considered a down-chirp filter. When the pulse duration, τ , falls within the limits $1.5(T\Delta f)^{0.5} \leq (T/\tau) \leq 0.25(T\Delta f)$, where $T=16.3 \mu\text{sec}$ is the total dispersive delay, and $\Delta f=100 \text{ MHz}$ is the bandwidth, then the output is a good approximation to a Fourier transform. The minimum frequency resolution is approximately equal to $(\Delta f/T)^{0.5}$, or 2.5 MHz for our SAW filter, although the finite pulse duration will cause a slightly poorer resolution.

The harmonic mixer system has also been used in conjunction with mode competition and multimode oscillation studies (Kreischer *et al.* 1984a). In this case, the rf signals of two modes simultaneously excited in the gyrotron were fed into the harmonic mixer at the same time. As a result of the strongly nonlinear behavior of the mixer, an IF signal was generated corresponding to the difference frequency $\Delta\omega$ of the two modes. The mixer was used both with and without an LO source. Use of an LO increased the sensitivity of the diagnostic but also increased the number of IF signals generated, making data interpretation more difficult. Using both of these approaches, $\Delta\omega$ in the range of 0 to 12.4 GHz were measured.

3. EXPERIMENTAL RESULTS

In this section, experimental data will be presented on the measured bandwidth of the 140 GHz gyrotron as well as on the dependence of the emission frequency on the operating parameters. Figure 2 shows an example of the output signal produced by the SAW filter. The peak shown corresponds to high efficiency operation in the $TE_{2,3,1}$ mode at 136.7 GHz. It represents the sideband obtained by mixing the rf emission with the 13th harmonic of the 10.5498 GHz LO frequency. Each small horizontal division in the trace corresponds to 1 μ sec, or a variation of 6.13 MHz of the IF signal entering the filter. Due to the down-chirp characteristic of the filter, a higher IF input would produce a peak with less delay, causing the signal in Fig. 2 to shift to the left. The peak shown has a FWHM of 0.75 μ sec, which implies a bandwidth of 4.6 MHz. This is slightly larger than the instrumental limit of the mixer system. Notice that the trace is quite clean, with little evidence of IF signals being produced by rf noise in the gyrotron. A sharp, narrow bandwidth is important if a gyrotron is to be used for scattering from plasma waves because the minimum plasma wave frequency that can be studied will be limited by the bandwidth. A scan in LO frequency indicated that for optimized operation in the $TE_{2,3,1}$ mode, only signals corresponding to this mode were evident.

Bandwidth measurements were made for a variety of modes by sampling a 300 ns interval during the flattop portion of the pulse. It was found that when the operation of the gyrotron was optimized, bandwidths as low as 3 MHz were observed. These narrow bandwidths existed at both low and high output powers. The primary effect that determines the lower limit on bandwidth in our device is ripple on the cathode voltage, which we have measured as $\pm 0.5\%$. Based on the dependence of frequency on the voltage, which is approximately 7.5 MHz/kV according to Fig. 3, a minimum bandwidth of 3-4 MHz

would be expected. Bandwidths below 1 MHz could therefore be achieved by reducing the ripple on the cathode voltage supply.

The measured frequency pulling characteristics of the gyrotron are plotted in Figures 3 through 5. Figure 3 shows the dependence of the output frequency on the cathode voltage and resonator magnetic field for the $TE_{0,3,1}$ mode. The total frequency change observed is about 100 MHz. This range of frequency pulling is somewhat limited because the $TE_{0,3,1}$ mode is not excited over its full resonance bandwidth, a result of mode competition from the $TE_{2,3,1}$ at lower fields and from the $TE_{5,2,1}$ at higher fields. The fact that the two curves in Fig. 3 are mirror images can be explained in a qualitative way as follows. For a given beam current, the observed frequency shift resulting from changes of either the magnetic field B or the cathode voltage V_c is due to their effect on the cyclotron frequency $\omega_c = eB/\gamma m_e$, where $\gamma = 1 + V_c/511$ and V_c is in kV. Therefore, changes in B and V_c that leave ω_c unchanged result in no change of the emission frequency. In order to determine the dependence of the emission frequency on ω_c , nonlinear theory, as discussed in Section 4, is required. The data presented in Fig. 3 agrees with this explanation.

In Fig. 4 the dependence of the frequency on the beam current and magnetic field is presented for the $TE_{2,3,1}$ mode. In this case the cathode voltage was held fixed at 64 kV. It should be noted that the output power varied over a wide range while B was changed and the current and voltage were held fixed. Here one can see that the operating frequency is an increasing function of both magnetic field and current, and that the frequency changes continuously as the magnetic field is varied. This is in contrast to Fig. 5, which is a plot of the emission frequency for the $TE_{4,2,1}$ mode for a beam current of 3 A. Since the $TE_{4,2,1}$ is an isolated mode, the magnetic field can be varied over the full resonance region, and this has resulted in a large total frequency shift of 350 MHz. The interesting features of

this graph are the two frequency jumps that occur. We believe these are due to a window mismatch that may be trapping radiation between the cavity and output window. Since the window was designed to be matched to the $TE_{0,3,1}$ mode at 140 GHz, such a mismatch at the $TE_{4,2,1}$ frequency of 127.3 GHz is not a surprise. Therefore, the three separate curves in Fig. 5 may correspond to excitation of high Q modes in the transmission waveguide between the cavity and window. The 140-150 MHz separation of the centers of the curves approximately agrees with the anticipated frequency difference $\Delta f = c/2L$ between these modes, where L is the length of the transmission waveguide, which in our case is 0.8 m.

4. THEORY

In this section, the frequency pulling measurements made on the 140 GHz gyrotron will be compared with predictions based on both linear theory and self-consistent nonlinear theory. Using linear theory (Kreischer and Temkin 1980), an expression can be derived for the percentage change in operating frequency $\Delta\omega/\omega$ that occurs when the resonator magnetic field is changed by a certain percentage $\Delta B/B$. This expression will be valid when the beam current is equal to the starting current and the gyrotron is operating in the linear regime. By comparing this theory with actual frequency measurements, we hoped to determine at what currents the linear theory becomes inadequate and nonlinear theory is required. If a Gaussian axial rf field profile $\exp(-2z/L)^2$ is assumed, the operating frequency ω can be expressed as

$$\frac{Q_T(\omega - \omega')}{\omega} = \frac{\left[D\left(\frac{x}{\sqrt{2}}\right) - \frac{1}{2}s\beta_{\perp}^2 D'\left(\frac{x}{\sqrt{2}}\right) \right]}{\sqrt{\pi}e^{-x^2/2} \left(1 + \frac{1}{2}s\beta_{\perp}^2 x\right)} \quad (1)$$

where Q_T is the total cavity Q, ω' is the cavity frequency without the beam present, $D(y)$ is Dawson's integral (Abramowitz and Stegun 1965), $x = L(\omega_c - \omega)/2v_{\parallel}$ is the detuning parameter, $s = \omega_c L/2v_{\parallel}$, and $\beta_{\perp} = v_{\perp}/c$ where v_{\perp} and v_{\parallel} are the perpendicular and parallel velocities respectively. Defining the right side of the above equation as $P(x)$, the change of operating frequency due to changes of the magnetic field can be written as

$$\frac{(\Delta\omega/\omega)}{(\Delta B/B)} = \frac{dP(x)}{dx} \left(\frac{s}{Q_T}\right) \quad (2)$$

where x is evaluated for the appropriate value of B . This equation has been used to obtain Fig. 6. In this graph, the relative change in ω as B is varied is shown as a function of s and x . The strongest frequency pulling occurs near the edges of the excitation region, for $x \geq -1$ or $x \leq -2.5$. Frequency pulling also increases as s increases, that is, as the axial

profile is broadened or v_{\parallel} is reduced. As one would expect, $\Delta\omega$ is inversely proportional to Q_T .

A simple expression can be obtained for the expected linear frequency pulling at the minimum starting current. If one assumes that $s\beta_{\perp}^2 \gg 1$, which is typically true, then the minimum starting current occurs at $x = x_{min} \simeq -1$. In this case, D' will dominate in the numerator of Eq.(1), and one can derive the approximation $P(x) \simeq D'(1/\sqrt{2})$. Substituting this into Eq.(2), and using $D''(0.71) = 1.4$, one can obtain the simple expression

$$\frac{(\Delta\omega/\omega)}{(\Delta B/B)} \simeq \frac{1.4s}{Q_T} \quad (3)$$

For our experiment, the design parameters were $L=1.53$ cm and $\beta_{\parallel}=0.384$, which yields an s of 87.6, and a total Q of 1380. According to Eq.(3), this gives a shift $(\Delta\omega/\omega)/(\Delta B/B)$ of 0.089 at x_{min} , which is in good agreement with the exact value of 0.072 that is obtained from Fig.(6). Unfortunately, these values are substantially higher than those observed experimentally. Although the curves for the $TE_{2,3,1}$ mode in Fig.(4) do have the characteristic 's' shape predicted by Fig.(6), this data indicates an approximate shift of 0.02 at $x \simeq -1$ for a beam current of 1 A, with slightly higher shifts occurring at higher currents. The minimum shifts, which occur in the middle of the excitation region, range from 0.011 for a current of 1 A, to 0.022 for 5 A, still well below the predicted value of 0.051 from Fig.(6). Data was taken as low as 0.5 A, which is twice the starting current, and the observed shifts were still well below theoretical predictions. This comparison therefore indicates that even at the relatively low power levels associated with operation at 0.5-1 A, linear theory does not adequately described the frequency pulling of the gyrotron.

A computer code developed by Fliflet (Fliflet *et al.* 1982) that is based on the non-linear, self-consistent interaction of the beam and rf field has been used to calculate the dependence of the emission frequency on the current and magnetic field. The input for

this program includes the dimensions of the gyrotron, which must have a weakly irregular axial profile so that no mode conversion occurs, and beam parameters such as the velocity components, current, and radius. An axial rf profile consistent with the electron beam presence in the cavity is then calculated along with the efficiency of the interaction, the output frequency, and the diffractive Q. This process is iterated until the rf field boundary conditions at each end of the resonator are satisfied. Assuming a cathode voltage of 64 kV, a v_{\perp}/v_{\parallel} of 1.5, and a beam radius of 1.82 mm, a plot of the theoretical emission frequency for the $TE_{2,3,1}$ mode, similar to the experimental plot shown in Fig.(4), has been obtained and is shown in Fig.(7). A comparison of these two graphs indicates an overall agreement, with the frequency increasing in both cases as the current and field are raised. The curves in Fig.(7) appear to have an almost linear dependence on B, especially at higher currents, which contrasts with the experimental results of Fig.(4). Unfortunately, a detailed comparison is not possible because the dependence of some beam parameters, such as v_{\perp} and v_{\parallel} , on the current, voltage, and field is not presently known with sufficient accuracy. The theoretical shifts $(\Delta\omega/\omega)/(\Delta B/B)$ shown in Fig.(7) range from 0.03 to 0.04. This is still somewhat high compared to the experimental results, but is in much better agreement than the value of about 0.08 based on linear theory.

5. CONCLUSIONS

Accurate measurements of the emission frequency and bandwidth of a 140 GHz pulsed gyrotron have been made. This data indicates that the gyrotron is capable of generating narrow band radiation at both low and high power. We have observed bandwidths as low as 3 MHz, which is the instrumental limit of the diagnostic system. It is likely that the primary lower limit of bandwidth for our device is due to the $\pm 0.5\%$ ripple on the cathode voltage, which causes a fluctuation of the output frequency. Based on the measured dependence of frequency on this voltage, a limit of 3-4 MHz would be expected. Therefore, bandwidths below 1 MHz appear feasible if fluctuations of the cathode voltage and magnetic field can be carefully controlled. The sharp, narrow bandwidths that were observed in our experiment, as well as the lack of rf noise being generated by the tube, indicate that the gyrotron can be used as a source for plasma diagnostic purposes, such as for Thomson scattering.

These high frequency measurements were made possible by a harmonic mixer system used in conjunction with a SAW filter. The SAW filter receives the amplified intermediate frequency from the mixer, and disperses the signal so that the relative delay of the output signal is a linear function of the frequency. This output can then be viewed on an oscilloscope in real time. For our system, a range of IF from 370 to 470 MHz can be viewed with each pulse. This diagnostic, besides being sensitive and capable of detecting weak modes excited in the gyrotron, allows frequency measurements accurate to a few MHz to be made on each pulse. This is in contrast to Fabry-Perot measurements, which require averaging over a large number of shots. In this case, bandwidth measurements can be erroneous if there are shot to shot fluctuations of the frequency.

In addition to measuring the bandwidth, the mixer system was used for a variety of other purposes. Due to its sensitivity, the mixer allowed us to determine the purity of

the output radiation and identify parasitic modes that were weakly excited simultaneously with the primary mode. It was found that when the operation of the device was optimized, only the main mode was excited. This confirmed that high efficiency and high power could be obtained in our device with single mode emission. The dependence of the emission frequency on device parameters was also investigated. It was found that for a fixed beam current and mode, the frequency shift due to variations of either the magnetic field or cathode voltage was the result of their effect on the cyclotron frequency. Another unique use of this diagnostic system was the identification of multimode oscillations, a potentially severe problem for our oversized cavity with its dense mode spectrum. In this case, the rf signals of two modes simultaneously present in the gyrotron were fed into the mixer, which generated a signal corresponding to the difference frequency of the two modes. Details of this work can be found in a recent paper (Kreischer *et al.* 1984a).

The experimental frequency pulling data was compared with predictions based on both linear and self-consistent nonlinear theory. A simple expression was derived for the percentage shift in frequency expected when the magnetic field was varied for beam currents close to the starting current. The shifts calculated based on this linear theory proved to be larger than the observed shifts, even for currents as low as 0.5 A. A comparison was then made with predictions based on self-consistent nonlinear theory. In the case of the $TE_{2,3,1}$ mode, a general agreement was found, with the frequency increasing as the current or magnetic field were raised. However, the nonlinear theoretical shifts were still larger than those observed experimentally, although in better agreement than the linear predictions. One problem that distorts the data for some modes is the mismatch of the rf window to the radiation. The window is matched to the $TE_{0,3,1}$ mode at 140 GHz, and becomes more poorly matched as the operating frequency decreases, reaching an extreme

for the $TE_{4,2,1}$ mode at 127 GHz. For this mode, abrupt frequency shifts occurred as the field was varied, suggesting that quasi-modes may be forming between the cavity and window. In spite of such mismatches, good powers and efficiencies were still achieved for modes such as the $TE_{4,2,1}$ (Kreischer *et al.* 1984).

Acknowledgements: This research was conducted under U.S.D.O.E. contract DE-AC02-78ET-51013. We are grateful to the Francis Bitter National Magnet Laboratory and the National Science Foundation for the use of their high field Bitter magnet and facilities. We also thank D.R. Cohn for his support throughout this work.

REFERENCES

Abramowitz, M., and Stegun, I., 1965. Handbook of mathematical functions. (New York :Dover Publications), 319.

Alikaev, V.V., et al., 1983. Plasma heating in the T-10 at the second ECR harmonic. Sov. J. Plasma Phys., **9**, 196-200.

Brand, G.F., Douglas, N.G., Gross, M., Ma, J.Y.L., and Chen, Z., 1983. Frequency detuning measurements in a low-power gyrotron. International Journal of Infrared and Millimeter Waves, **4**, 891-900.

Byerly, J.L., Danly, B.G., Kreischer, K.E., Temkin, R.J., Mulligan, W.J., and Woskoboinikow, P., 1984. Harmonic emission from high-power high-frequency gyrotrons. To be published in this issue.

Cohn, D.R., Gerver, M., Post, R.S., Temkin, R.J., and Woskoboinikow, P., 1983. Use of high frequency gyrotron radiation for collective scattering in TARA. Bull. American Phys. Soc., **28**, 1181.

Fetterman, H.R., Tannenwald, P.E., Parker, C.D., Melngailis, J., Williamson, R.C., Woskoboinikow, P., Praddaude, H.C., and Mulligan, W.J., 1979. Real-time spectral analysis of far-infrared laser pulses using a SAW dispersive delay line. Appl. Phys. Lett., **34**, 123-125.

Fiks, A.Sh., Flyagin, V.A., Luchinin, A.G., Nusinovich, G.S., and Shishkin, B.V., 1984. Powerful gyrotrons for electron cyclotron resonance heating and active diagnostics of plasmas. Conf. Heating in Toroidal Plasmas, Rome, Italy.

Fliflet, A.W., Read, M.E., Chu, K.R., and Seeley, R., 1982. A self-consistent field theory for gyrotron oscillators: application to a low Q gyromonotron. International Journal of Electronics, **53**, 505-522.

Gaponov, A.V., Flyagin, V.A., Goldenberg, A.L., Nusinovich, G.S., Tsimring, Sh. E., Usov, V.G., and Vlasov, S.N., 1981. Powerful millimetre-wave gyrotrons. International Journal of Electronics, **51**, 277-302.

Hsuan, H., Bol, K., Bowen, N., Boyd, D., Cavallo, A., Dimits, A., Doane, J., Elder, G., Goldman, M., Grek, B., Hoot, C., Johnson, D., Kritz, A., Leblanc, B., Manintveld, P., Polman, R., Sesnic, S., Takashashi, H., and Tenney, F., 1984. Major results of the electron cyclotron heating experiment in the PDX tokamak. Fourth Int. Symp. on Heating in Toroidal Plasmas, Rome, Italy.

Kreischer, K.E., and Temkin, R.J., 1980. Linear theory of an electron cyclotron maser operating at the fundamental. International Journal of Infrared and Millimeter Waves, **1**, 195-223.

Kreischer, K.E., Temkin, R.J., Fetterman, H.R., and Mulligan, W.J., 1984a. Multimode oscillation and mode competition in high frequency gyrotrons. IEEE Transactions on

Microwave Theory and Techniques, **32**, 481-490.

Kreischer, K.E., Schutkeker, J.B., Danly, B.G., Mulligan, W.J., and Temkin, R.J., 1984b. High efficiency operation of a 140 GHz pulsed gyrotron. To be published in this issue.

Temkin, R.J., Kreischer, K.E., Mulligan, W.J., MacCabe, S., and Fetterman, H.R., 1982a, A 100 kW, 140 GHz gyrotron. International Journal of Infrared and Millimeter Waves, **3**, 427-437.

Temkin, R.J., Woskoboinkow, P., Cohn, D.R., Kreischer, K.E., Mulligan, W.J., and Fetterman, H.R., 1982b. High frequency gyrotrons for plasma diagnostic applications. Bull. Am. Phys. Soc., **27**, 836.

Woskoboinkow, P., Cohn, D.R., and Temkin, R.J., 1983. Application of advanced millimeter/far infrared sources to collective Thomson scattering plasma diagnostics. International Journal of Infrared and Millimeter Waves, **4**, 205-229.

FIGURES

Figure 1 Schematic of harmonic mixer system.

Figure 2 Output signal from SAW filter for high efficiency operation in the $TE_{2,3,1}$ mode.

Figure 3 Dependence of emission frequency on cathode voltage and resonator magnetic field for the $TE_{0,3,1}$ mode.

Figure 4 Dependence of emission frequency on beam current and cathode voltage for the $TE_{2,3,1}$ mode.

Figure 5 Measured emission frequency for the $TE_{4,2,1}$ mode. This data suggests the possibility of a window mismatch.

Figure 6 Predicted frequency pulling based on linear theory versus x and $s = \omega_c L / 2v_{\parallel}$.

Figure 7 Theoretical frequency pulling for the $TE_{2,3,1}$ mode based on self-consistent non-linear theory.

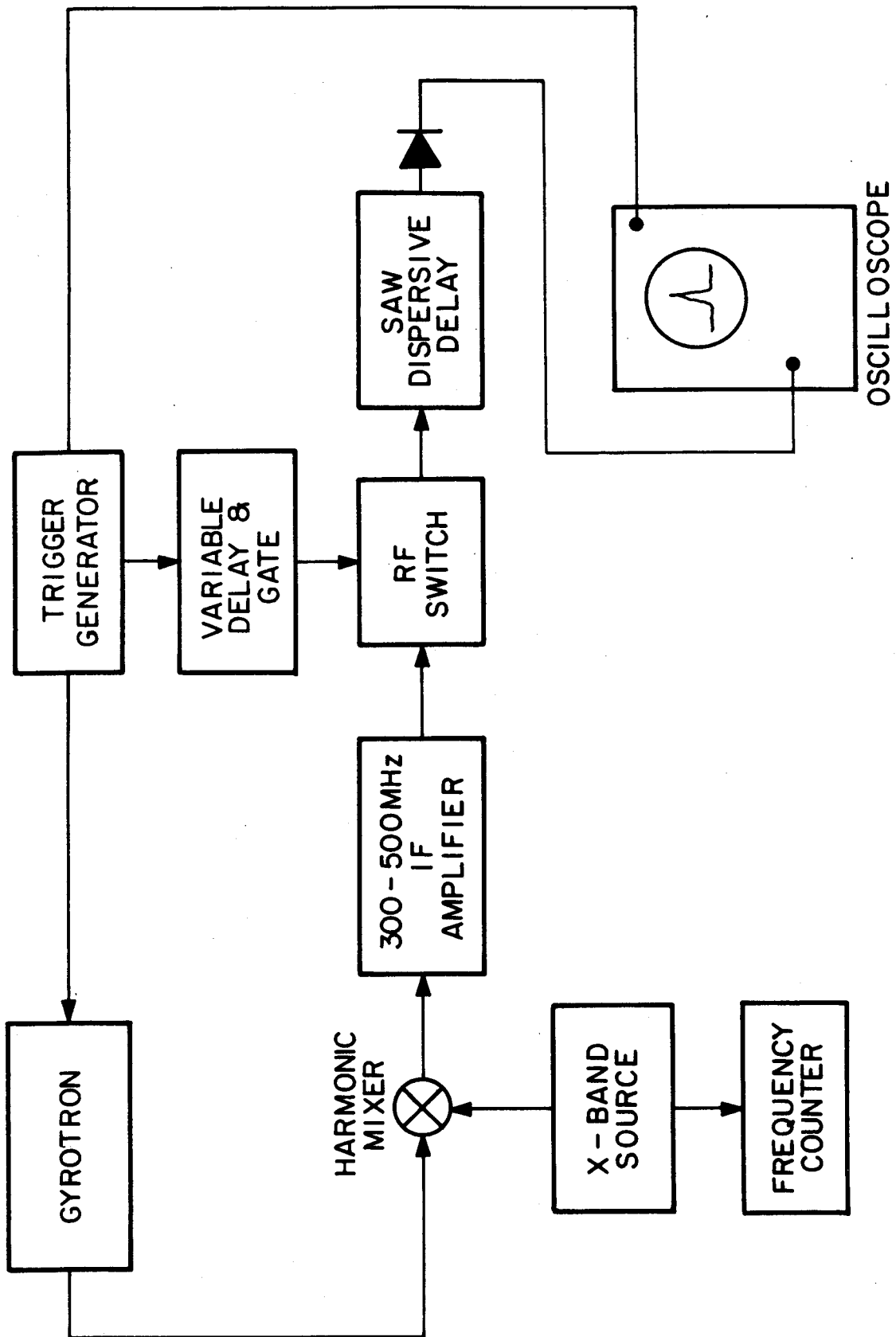


Figure 1

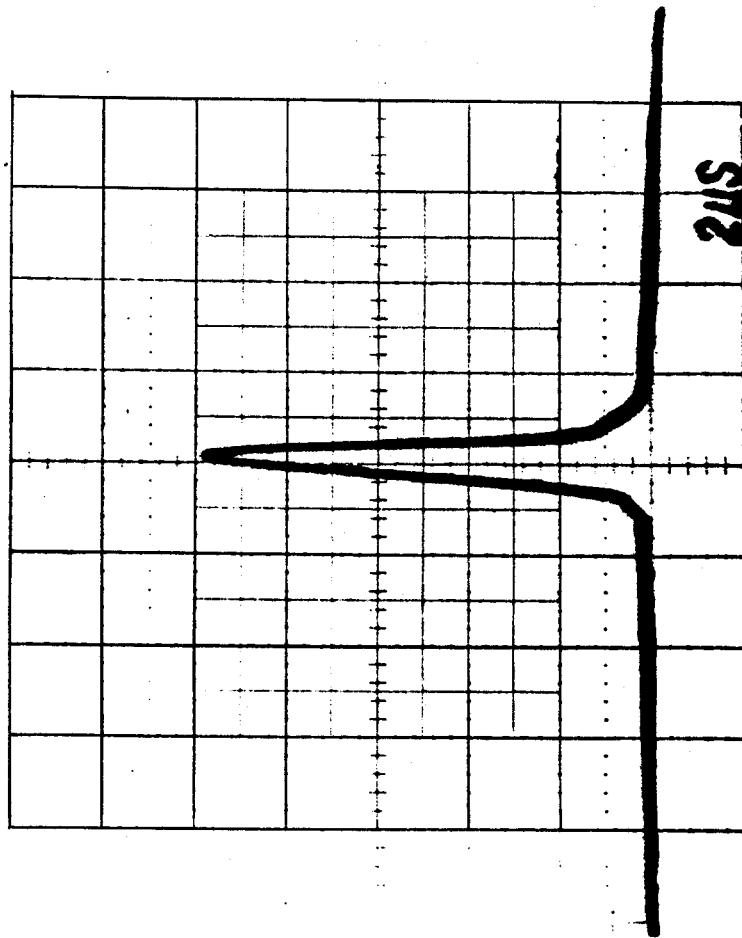


Figure 2

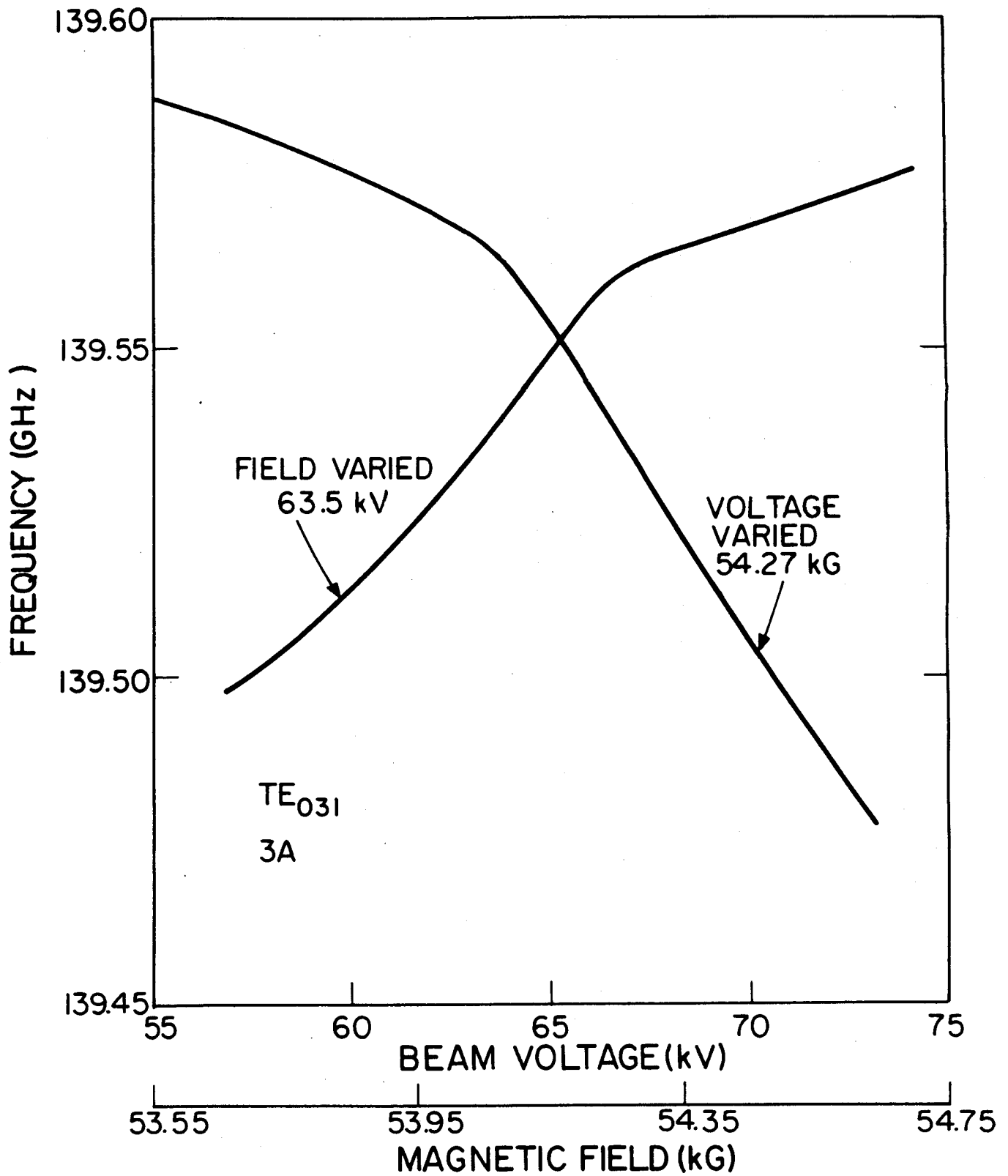


Figure 3

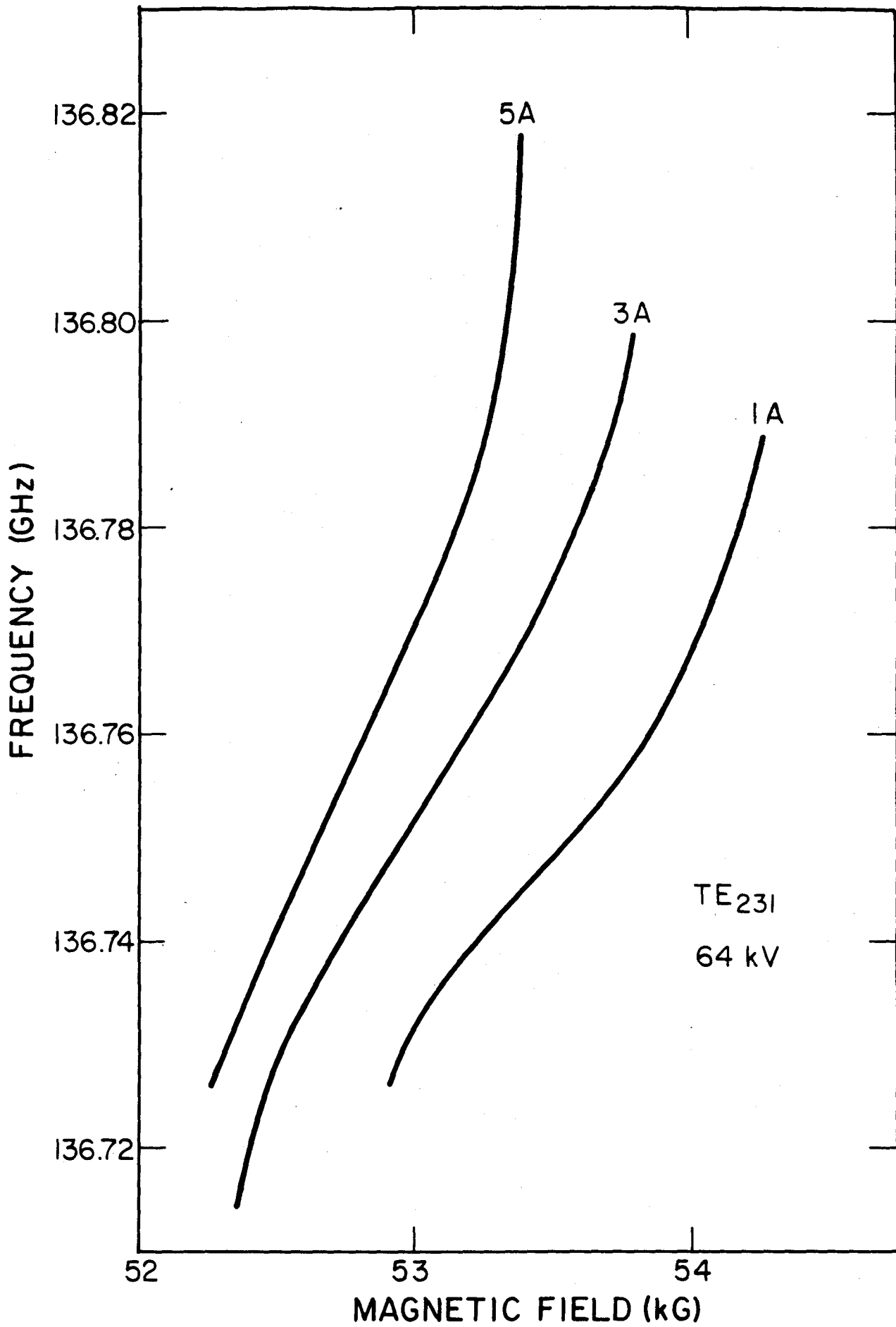


Figure 4

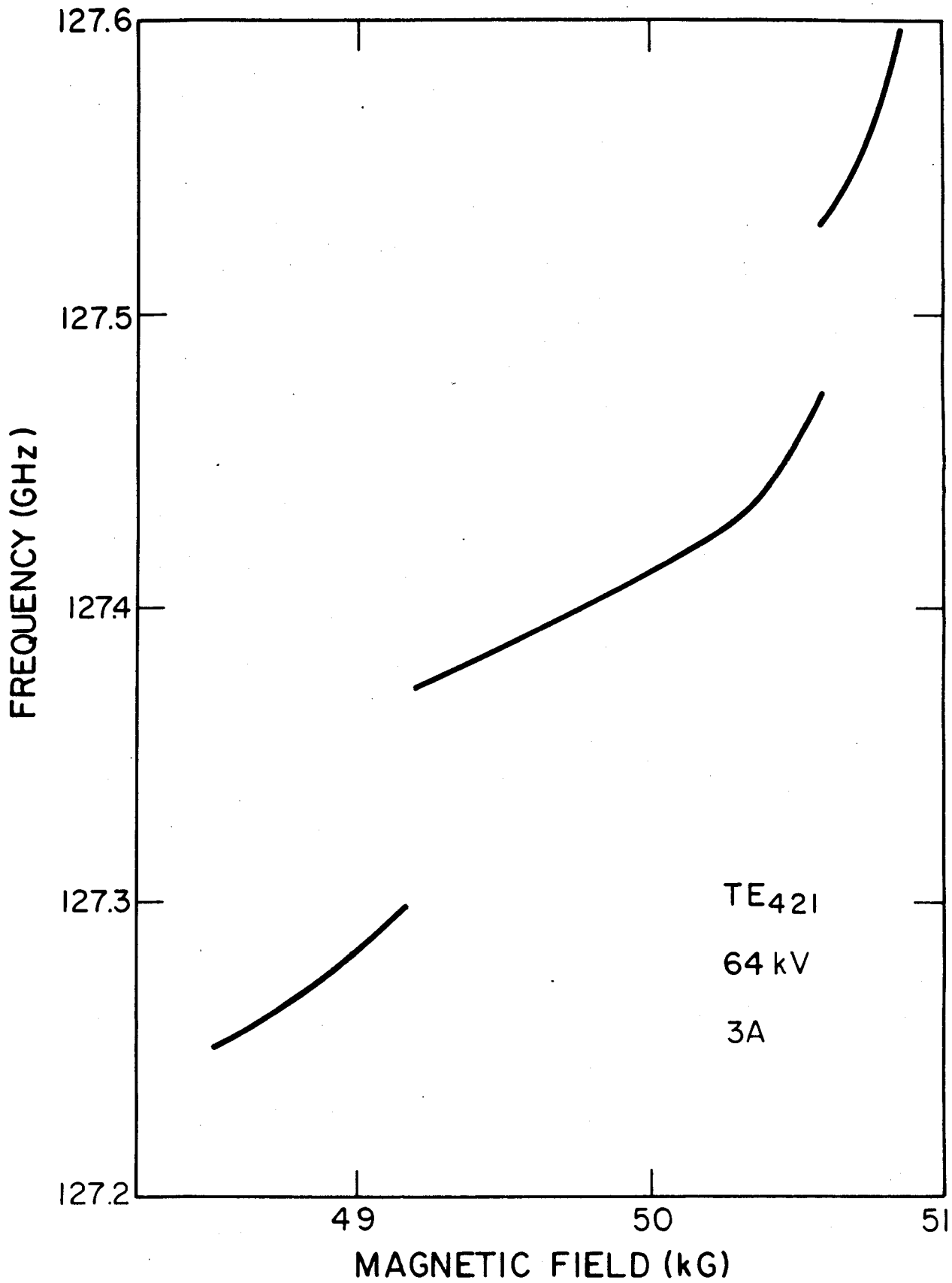


Figure 5

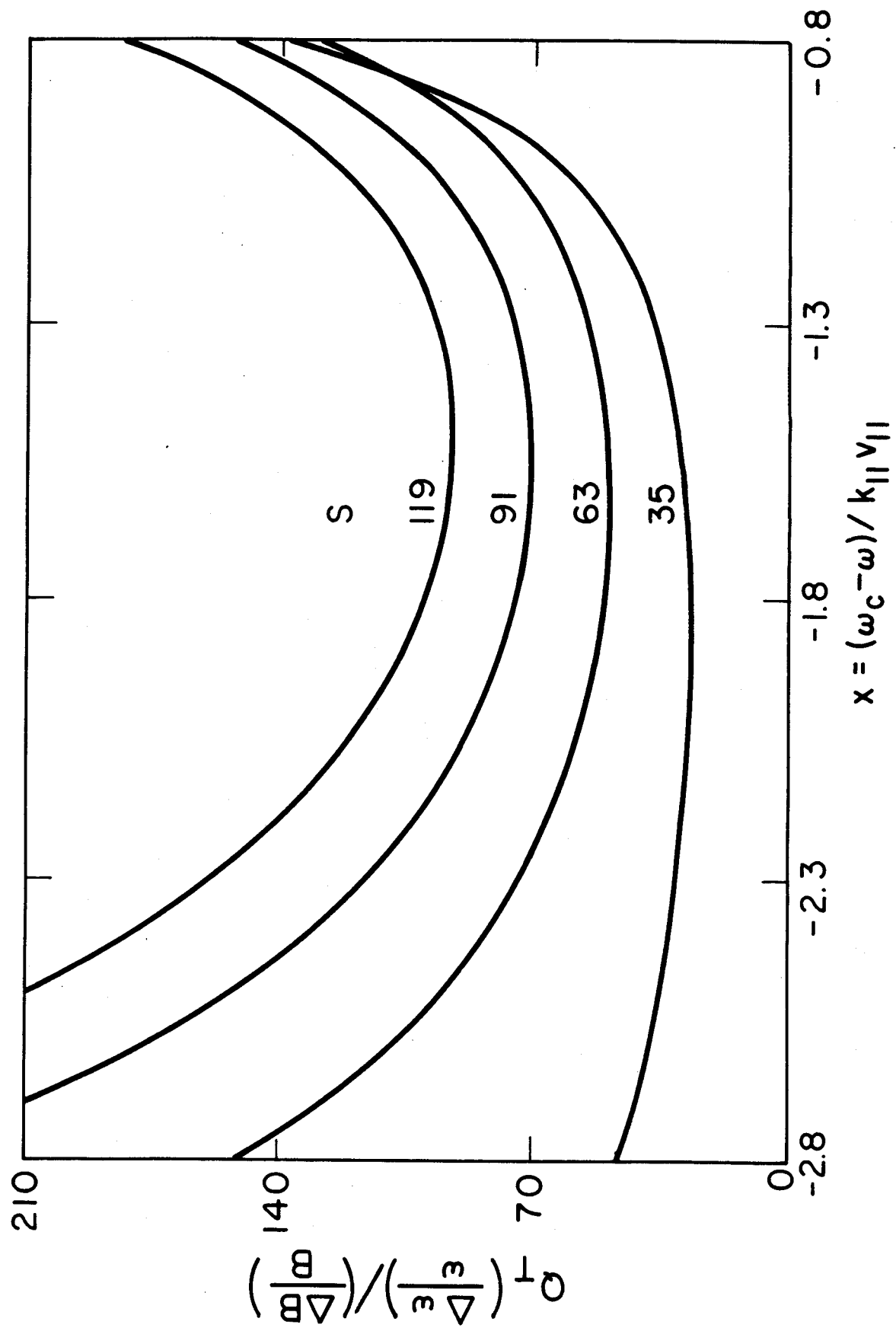


Figure 6

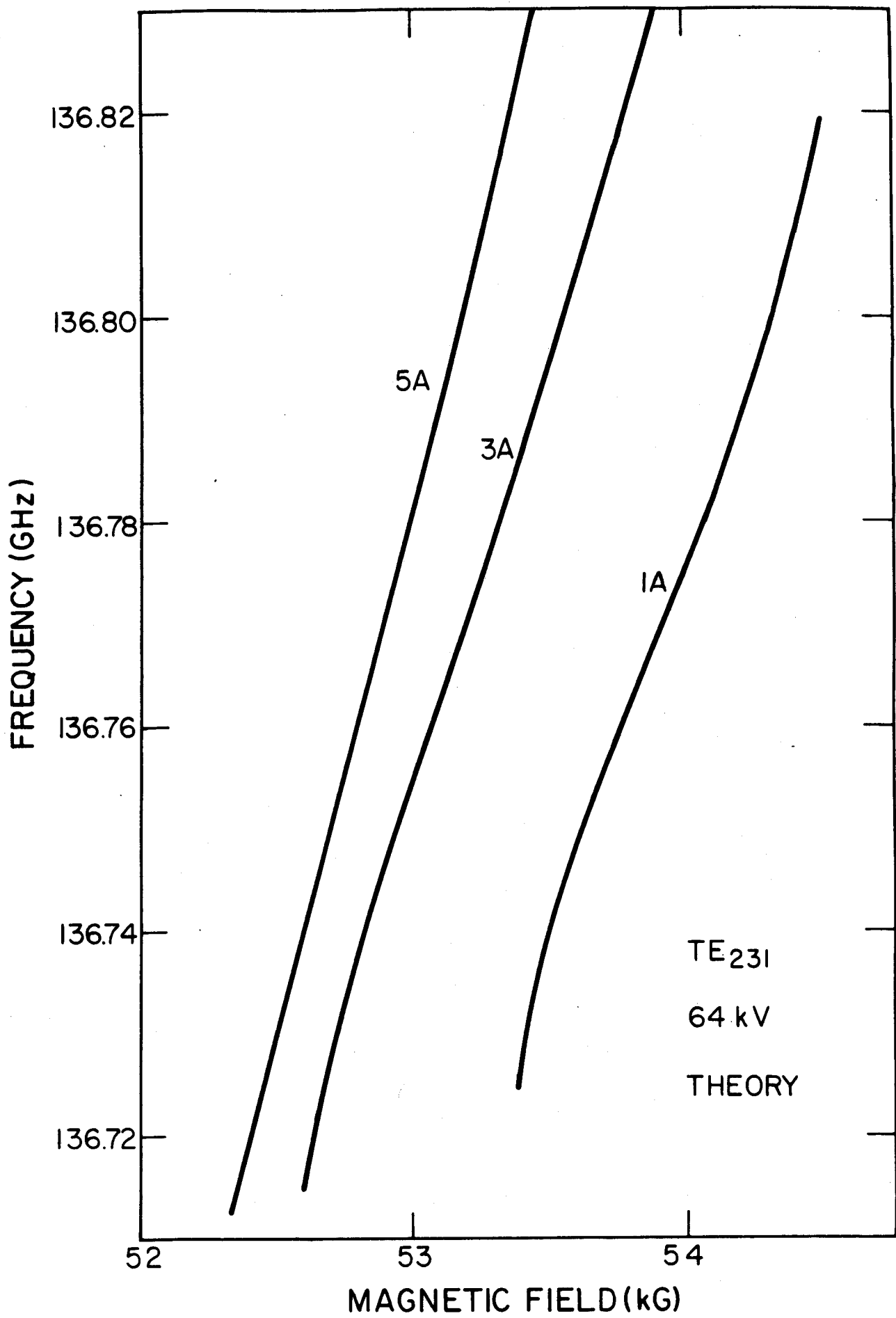


Figure 7